



# Morphological and molecular variability of *Peridinium volzii* Lemmerm. (Peridiniaceae, Dinophyceae) and its relevance for infraspecific taxonomy

Victoria J. C. Holzer<sup>1</sup> · Juliane Kretschmann<sup>1</sup> · Johanna Knechtel<sup>1</sup> · Paweł M. Owsianny<sup>2</sup> · Marc Gottschling<sup>1</sup>

Received: 26 March 2021 / Accepted: 16 August 2021  
© The Author(s) 2021

## Abstract

Contemporary delimitation of species and populations in the microbial domain relies on an integrative approach combining molecular and morphological techniques. In case of the dinophyte *Peridinium volzii*, a considerable number of infraspecific taxonomic entities have been reported, but it is unclear at present whether the corresponding traits are stable within reproductively isolated units or refer to intraspecific variability. We established 26 monoclonal strains from Central Europe with a morphology that is consistent for *P. volzii* and characterised them by sequences gained from the rRNA operon. Ten of such strains, representative for the entire diversity observed, were investigated in detail morphologically using light and electron microscopy. In the molecular tree, *P. volzii* was monophyletic, sister group of *Peridinium willei*, and three ITS ribotypes could be distinguished. Some traits corresponding to previously described varieties and forms were found in individual cells across the strains under investigation, but not as stable characters correlating to certain ribotypes. We also observed new morphological variability (e.g., unusual shape of plate 4"). Cell size and displacement of the cingulum were significantly different between certain ribotypes but in turn, such diagnostic traits are impossible to assign to already described taxa due to their ambiguity. Based on the small first apical plate as diagnostic trait and putative apomorphy, *P. volzii* is a characteristic species but the present data given, we are reserved to accept more than a single reproductive unit. Thus, more research is necessary, including a focus on species delimitation to putative close relatives such as *Peridinium maeandricum*.

**Keywords** Dinoflagellate · Molecular phylogenetics · Morphology · rRNA · Taxonomy · Theca

## Introduction

Dinophytes play an equally important role in the ecology of water bodies, although they are not as visually apparent as larger aquatic organisms. Habitat preference is clearly marine, but they are also known to be widely distributed in freshwater (Moestrup & Calado, 2018). As unicellular algae and important bioindicators in aquatic systems, they have the ability to indicate rapid environmental changes within these habitats (Camargo, 1994; Hellowell, 1986). The adaptability

upon exposure to environmental and anthropogenic stressors is enabled by a high degree of plasticity in the morphology and molecular constitution (Chevin et al., 2010; Wong & Candolin, 2015) also of dinophytes. However, knowledge of intraspecific variability is currently limited, hindering proper monitoring of unicellular organisms and their ecological impact (Gottschling et al., 2020).

Generally accepted criteria for species delimitation are absent for unicellular organisms such as dinophytes (Boenigk et al., 2012; Mayr, 1982a, b). Crossing experiments are the first choice to test reproductive isolation of populations, but are challenging and therefore rare in dinophytes (Blackburn et al., 2001; Figueroa et al., 2010; Pfister & Skvarla, 1979; Soyer-Gobillard et al., 2002). The morphological species concept is still very viable for such organisms. However, the quality of a diagnostic trait and its abundance in a certain population is not easy to work out precisely as well. This is especially true for character states that have been used to describe taxa at the

✉ Marc Gottschling  
gottschling@bio.lmu.de

<sup>1</sup> Department Biologie: Systematics, Biodiversity & Evolution of Plants, GeoBio-Center, Ludwig-Maximilians-Universität München, Menzinger Str. 67, München, Germany

<sup>2</sup> Nadnotecki Institute UAM in Piła, Adam Mickiewicz University, ul. Kołobrzeska 15, Piła, Poland



various infraspecific ranks such as varieties (var.) and forms (forma). DNA sequencing has become an important tool to help resolve taxonomic issues (Blaxter, 2004; Keck et al., 2018; Kretschmann et al., 2018b; Miller, 2007). Contemporary delimitation of species and populations in the microbial domain therefore relies on an integrative approach combining molecular and morphological techniques. Anyhow, evaluation of any scientific name of microbes described prior to the last millennium has some uncertainty, as it lacks DNA sequence information (Boenigk et al., 2012; De Clerck et al., 2013; Romeikat et al., 2019).

The freshwater dinophyte *Peridinium volzii* Lemmerm. is no exception, as it includes both a rather high degree of morphological variation and a considerable number of infraspecific taxa (Lefèvre, 1932; Lindemann, 1920; Moestrup & Calado, 2018). Supposedly unaware of E. Lemmermann's description, Lindemann (1916) described the morphologically similar *Peridinium guestrowiense* Er.Lindem., which is today regarded as synonymous with *P. volzii*. Early in history, the species was considered as a junior synonym of *Peridinium willei* Huitf.-Kaas, as their thecal plate pattern is highly similar (Lindemann, 1917; Playfair, 1920), and this assumption persisted until our times (Popovský & Pfister, 1990). Both species share the plate formula of *Peridinium* Ehrenb. (4', 3a, 7'', 5''', 2''''': Izquierdo López et al., 2018; Moestrup & Calado, 2018). *Peridinium volzii* and *P. willei* are further characterised by the symmetric arrangement of epithelial plates, a sulcus that extends towards the hypotheca, the absence of an apical pore and plate 1' not abutting the pentagonal plate 3'.

Today, two separated species are accepted constituting the *P. willei* species group (Bachmann, 1911; Moestrup & Calado, 2018), and *P. volzii* can be distinguished from *P. willei* based on its considerably smaller plate 1'. Additionally, *P. volzii* differs from *P. willei* by a sulcal extension on the epitheca being longer than wide and not shorter than wide, as well as the absence of hyaline wings on the epitheca (Lindemann, 1920: 146; Moestrup & Calado, 2018). It also appears that ecological differences separate these two species, with *P. volzii* having more narrow seasonal and pH limits (Ollrik, 1992). The occurrence of *P. volzii* in the plankton seems to be restricted from late-spring to summer in calcium-rich lakes and ponds, rarer in other types of waters (Höll, 1928). Moreover, *P. willei* occurs in ponds and lakes with transparent through polyhumic brownish water, while *P. volzii* is mainly found in the plankton of calcium-rich ponds and lakes avoiding humic water. The distinctiveness between *P. volzii* and *P. willei* is also displayed in molecular phylogenetic trees (Gottschling et al., 2020; Hayhome & Pfister, 1983; Ki et al., 2011).

*Peridinium volzii* is considered a morphologically variable species, and seven infraspecific taxa are currently accepted (Moestrup & Calado, 2018). Traits that have been used for

the taxonomic assessment of the intraspecific variability are deviations from the general cell shape [*Peridinium volzii* forma *compressum* (Er.Lindem.) M.Lefèvre], cell ornamentation [*Peridinium volzii* var. *maeandricum* (Lauterborn) Er.Lindem.], plate shape [*Peridinium volzii* forma *cyclicum* (Er.Lindem.) M.Lefèvre] or presence of additional sutures (*Peridinium volzii* forma *complexum* Krakhmalny). Further traits to segregate infraspecific taxa are size (*Peridinium volzii* var. *maximum* C.Bernard), width of the sutures (*Peridinium guestrowiense* forma *late-intercalatum* Er.Lindem.) and fusion of plates (*Peridinium volzii* var. *simplex* M.Lefèvre). In the original description of *P. volzii* from Singapore, Lemmermann (1905) noted the presence of a distinct antapical spine, which is however absent from those infraspecific taxa (or supposed synonyms such as *P. guestrowiense*) described from Central Europe (Lefèvre, 1927; Lindemann, 1916, 1919, 1920).

*Peridinium volzii* appears morphologically highly variable, but no DNA sequence data are linked to the infraspecific and putatively synonymous names assigned to the species. In turn, the DNA sequence of only a single strain (NIES501; Ki et al., 2011) is available, though without knowledge of morphology. In this study, we present the first integrative approach to understand intraspecific variability in *P. volzii*, providing both morphological and molecular data of newly established monoclonal strains. We show already assessed morphological variation, but also new traits yet not been described in the literature, and the existence of three ITS ribotypes. In the phylogenetic tree, *P. volzii* and *P. willei* are clearly delimited species within the Peridiniaceae. We aim at a better knowledge of intraspecific variability within dinophyte species, which may have importance also for other microalgal groups.

## Material and methods

### Cultivation and microscopy

During field trips in Germany and Poland, water tow samples were collected using a plankton net with a mesh size of 20 µm. Motile cells were isolated and placed in 24-well microplates (Thermo Fisher Scientific; Waltham, USA) and later in cell culture bottles with filter screw cap (Roth; Karlsruhe, Germany) filled with WC medium (Guillard & Lorenzen, 1972) under sterile conditions. The plates and cell culture bottles were stored in a climate chamber either at constant 18 °C (WKS 3200, Liebherr; Bulle, Switzerland; strains GeoM\*787, GeoM\*788, GeoM\*789, GeoM\*793, GeoM\*794 and GeoM\*866) or 12 °C Percival I-36VL (CLF Plant Climatics; Wertingen, Germany; strains GeoK\*024, GeoK\*026, GeoK\*037 and GeoK\*044). Cells were exposed to 80 µmol photons m<sup>-2</sup> s<sup>-1</sup> under a 12:12 h light:dark cycle.

Detailed information of the localities and collectors are compiled in Table S1.

Thecate cells were observed under an inverse light microscope (LM) CKX41 (Olympus; Hamburg, Germany). Documentation was performed with a DP73 digital camera (Olympus) and subsequent cell size measurements using the software cellSense (Olympus). Measurements were taken in LM using selected strains representative for the observed diversity. Statistically significant clusters were calculated with Tukey's Honest Significant Difference (HSD) test ( $p$ -values < 0.05) and illustrated using the R software v4.0.3 (freely available under [www.r-project.org](http://www.r-project.org)).

For the preparation of permanent slides, cells were fixed with 2.5% glutar(di)aldehyde (agar scientific; Stansted, Essex, UK). Double-staining was carried out using 0.5% (water-based) astra blue in 2% tartaric acid (Fluka; Buchs, Switzerland) in WC medium and 0.1% (ethanol-based) eosin (Merck; Darmstadt, Germany) during a graded ethanol (Roth) series. Ethanol-based Technovit 7100 (Heraeus; Wehrheim, Germany) was used for embedding, following the manufacturer's instructions. For the final preparation, 30  $\mu$ l aliquots of the Technovit mixture including the embedded samples were transferred to three slides. The material is deposited at the Centre of Excellence for Dinophyte Taxonomy (CEDiT; Wilhelmshaven, Germany), and duplicates are held in Berlin, B and Munich, M.

Sample preparation for scanning electron microscopy (SEM) followed a standard protocol (Janofske, 2000), applied in several previous studies (Gottschling et al., 2012; Kretschmann et al., 2018a, 2020). The cells were fixed overnight using 2.5% glutar(di)aldehyde. The cells were filtered onto an Omnipore<sup>TM</sup>-membrane filter (5  $\mu$ m; Merck; Darmstadt, Germany), which was placed in a Swinnex<sup>®</sup> filter holder (Merck), and dehydrated with a graded acetone series. Critical point drying was followed by sputter-coating (BAL-TEC SCD 050 sputter coater; Schalksmühle, Deutschland) with platinum on an aluminium stub coated with Planocarbon (Plano; Wetzlar, Germany). Subsequent imaging was performed with the SEM LEO 438VP (LEO; Cambridge, UK) at 15 kV. Image adjustment and arrangement of LM and SEM pictures were done in Photoshop and InDesign (Adobe; Munich, Germany).

## Molecular phylogenetics

A systematically representative set of peridiniacean accessions was compiled, considering the information provided by dinophyte reference trees such as presented in Gottschling et al. (2020). The sample was enriched by all those sequences deposited in GenBank, which showed ultimately close relationships to the sequence data gained in the present study, as inferred from BLAST searches (Altschul et al., 1990). Full voucher information is

provided in Table S1, including information of the out-group comprising dinophytes of Heterocapsaceae and Protoperidiniaceae. The ITS sequences were also inspected for possible compensatory base changes that occur when substitutions take place in pairing regions of the molecule folded into a secondary structure (Gottschling & Plötner, 2004; Kremp et al., 2014; Thornhill & Lord, 2010).

For alignment constitution, separate matrices of the rRNA operon (i.e., SSU, ITS, LSU) were constructed, aligned using 'MAFFT' v6.502a (Kato & Standley, 2013) and concatenated afterwards. The aligned matrices are available as \*.nex files upon request. Phylogenetic analyses were carried out using maximum likelihood (ML) and the Bayes theorem, as described in detail previously (Gottschling et al., 2020) using the resources available from the CIPRES Science Gateway (Miller et al., 2010). The MPI version of 'RAxML' v8.2.4 (Stamatakis, 2014, freely available at <http://www.exelixislab.org/>) was applied using the GTR +  $\Gamma$  substitution model under the CAT approximation. We determined the best-scoring ML tree and performed 1,000 non-parametric bootstrap replicates (rapid analysis) in a single step. The Bayesian analysis was performed using 'MrBayes' v3.2.6 (Ronquist et al., 2012, freely available at <http://mrbayes.sourceforge.net/download.php>) under the GTR +  $\Gamma$  substitution model and the random-addition-sequence method with 10 replicates. We ran two independent analyses of four chains (one cold and three heated) with 20,000,000 generations, sampled every 1,000th cycle, with an appropriate burn-in (10%) as inferred from the evaluation of the trace files using Tracer v1.5 (<http://tree.bio.ed.ac.uk/software/tracer/>). Statistical support values (LBS: ML bootstrap support) were drawn on the resulting, best-scoring tree.

## Results

### Morphology of *Peridinium. volzii*

All investigated strains exhibited cells that were either flagellated (Fig. 1a, i) or coccoid (Fig. 1k–m), with the motile cells being predominant. Motile cells swam homogeneously within the medium or occasionally, they accumulated towards the light source. Each cell, except for necrotic cells, contained numerous gold- through olive-brownish chloroplasts and an orange to red accumulation body (Fig. 1i). An eyespot was absent. Necrotic cells included plastids that appeared grey through silver.

All strains were indistinguishable from each other in gross morphology, and motile cells were continuously covered by a theca built of cellulosic plates (as inferred from astra blue staining). Thecate cells had an ovoid shape and were slightly compressed dorso-ventrally. The hypotheca was generally smaller than the epitheca. Average cell sizes



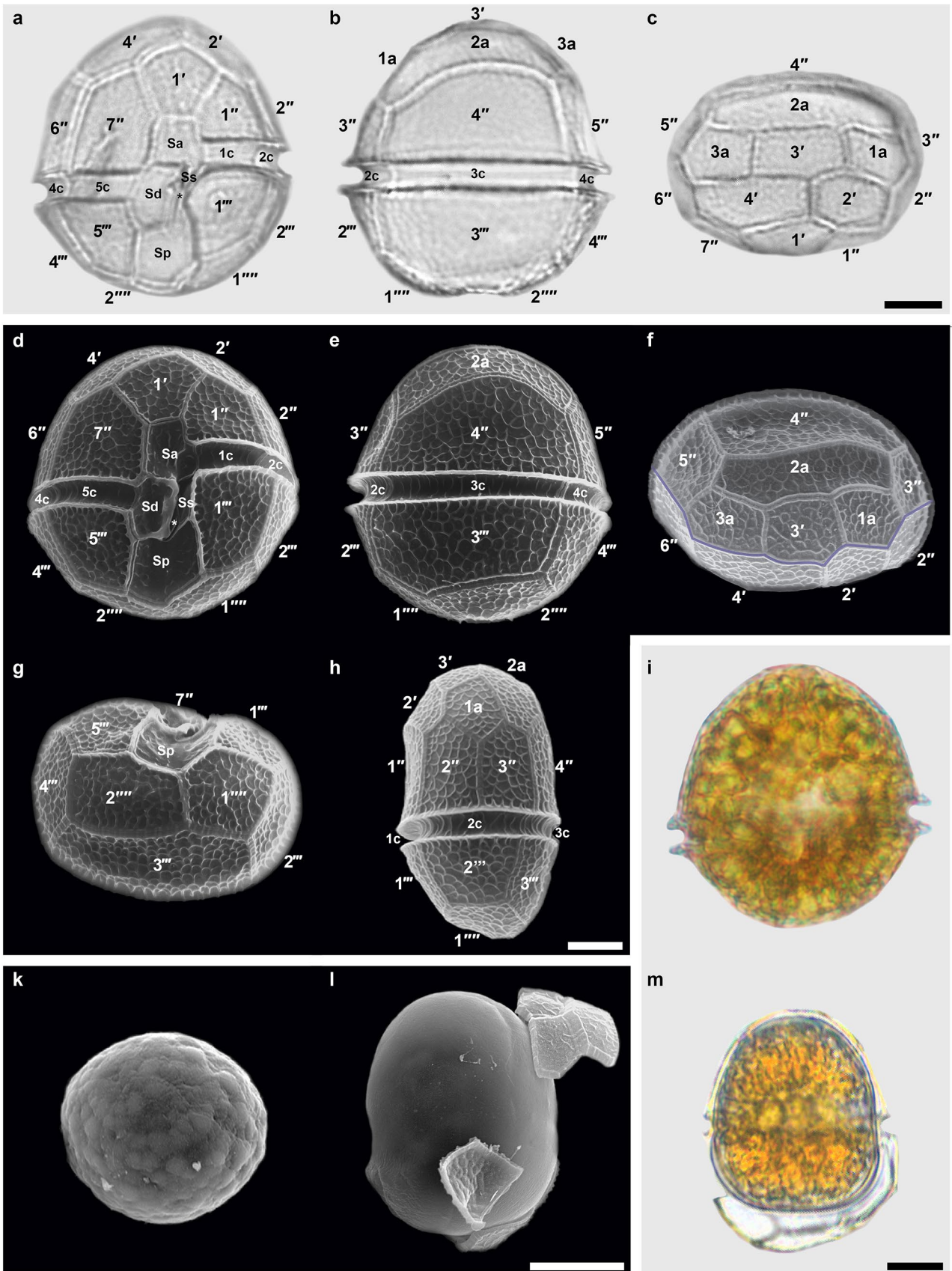


**Fig. 1** Morphology of thecate and coccoid cells, with labelled thecal plates. **a–c, i, m** Light microscopy, **d–h, k–l** scanning electron microscopy. **a** Ventral view of strain GeoM\*788; **b** dorsal view of strain GeoM\*793; **c** apical view of strain GeoK\*044; **d** ventral view of strain GeoK\*037; **e** dorsal view of strain GeoM\*788; **f** apical view of strain GeoK\*024, with the dehiscence of epithecal opening indicated by a blue line; **g** antapical view of strain GeoK\*044; **h** left-lateral view of strain GeoM\*866; **i** motile cell of strain GeoK\*037; **k–m** coccoid cells showing variability in shape and size of strains **k** GeoM\*866, **l** GeoM\*793 and **m** GeoK\*024. Abbreviations: n': apical plate, n'': precingular plate, n''': postcingular plate, n''': antapical plate, na: anterior intercalary plate, nC: cingular plate, Sa: anterior sulcal plate, Sd: right sulcal plate, Sp: posterior sulcal plate, Ss: left sulcal plate. Scale bar: 10  $\mu$ m.  $U_A$ : 15 kV

of motile cells within the ten strains under detailed study ranged from 41 to 51  $\mu$ m in length and from 36 to 48  $\mu$ m in width (Table 1). However, cell sizes of particular strains were significantly different from each other (Fig. 2a, b). All strains presented the thecal formula 4', 3a, 7'', 5c, 5s, 5''', 2''', with few exceptions (see below). The surface of the plates was strongly reticulate, and each major plate of the epi- and hypothecae contained one or two pores.

The epithecal plate pattern was largely symmetrical, although the apical plate 2' was always smaller than the apical plate 4' (Fig. 1a, c–d, f). The apical plate 1' appeared small, was rhomboid and ca 12–14  $\mu$ m tall. Two significantly different suture lengths between the plates 1' and 4' were distinguishable across the strains (Fig. 2c), being shorter (Fig. 1a) or longer (Fig. 1c–d). Both apical plates 2' and 4' appeared hexagonal in shape and plate 3' pentagonal. The apical plate 3' is separated from plate 1' by plates 2' and 4' and was either as wide as tall (Fig. 1f) or slightly wider than tall (Fig. 1c). The intercalary plates 1a and 3a were pentagonal, had the same size and were smaller than the elongated plate 2a (Fig. 1c, f).

Deviations from the archetypical plate pattern could be stated (Tables 1, 2 and 3). Usually tetragonal, precingular plate 4'' was occasionally pentagonal (Fig. 3a, b) and abutted plate 3a, from which it was otherwise separated. This conformation affected the position and size of the intercalary plate 2a, which appeared smaller and less elongated. In few individual cells of all strain, the intercalary plate 2a (Fig. 3c), the apical plate 3' (Fig. 3m) or the postcingular plate 3''' (Fig. 3i) were split, and also unusual fusions of plates could be observed (Table 3; Fig. 3d, f).

The cingulum was median or sub-median and descending. The displacement was significantly different between the strains (Table 1), with either ca 1 cingulum width (Fig. 1a) or ca 1.5–2 cingulum widths (Fig. 1d). Notably, this distinction correlated with the two different suture lengths between apical plates 1' and 4' (Table 1). The sulcus appeared narrow and extended into the epitheca for approximately a cingulum

width (Fig. 1a, d). Two flagella originated from the junction between sulcus and cingulum and were visible in LM.

Cell division was by eleutheroschisis. The resulting empty thecae were collected in high quantity at the bottom of the cultivation plate. The theca opened along the edge of the cingulum that epitheca and hypotheca were separated. The predominant opening of the epitheca was exhibited at the apical side between the three intercalary plates and the plates 2' and 4' (Fig. 1f). The cell opening continued at the sutures between the precingular plates 5'' and 6'' as well as 2'' and 3'', resulting in the release of the dorsal part of the epitheca. Subsequently, this thecal split led to the release of the ventral epitheca, as well as the separation of epitheca and hypotheca (Fig. 1m). This specific dehiscence line was present in all strains with a frequency of 66–82% (Table 1). Deviations from the regular opening line predominantly occurred at the precingular plates in all strains investigated. Sutures between thecal plates varied from thin lines through wide bands, the latter exhibiting cross striations (Figs. 1f, 3b, e, g).

Coccoid cells varied in their average size from 39 to 50  $\mu$ m in length and from 32 to 45  $\mu$ m in width (Table 1) and were either thecate or athecate. Their shapes were variable ranging from spherical through obovoid. Some coccoid cells exhibited a slight dorso-ventrally flattening (Fig. 1l). Within these cells, brown granules of varying sizes were observed in addition to the plate-like chloroplasts. A single coccoid cell was observed to develop intrathecatly (Fig. 1m), and the ecdysing cell was released by thecal opening along the edge of the cingulum.

## Molecular phylogenetics

The SSU + ITS + LSU alignment was 1,802 + 703 + 2,517 bp long and was composed of 311 + 351 + 467 parsimony-informative sites (22%, mean of 18.21 per terminal taxon) and 2,048 distinct RAxML alignment patterns. Figure 4 shows the best-scoring ML tree ( $-\ln = 22,017.62$ ), with the majority of nodes showing high if not maximal support. The Peridiniaceae were monophyletic (100LBS, 1.00BPP) and segregated into *Peridinium gatunense* Nygaard (single accession), *Peridinium cinctum* (O.F.Müll.) Ehrenb. (99LBS, 1.00BPP), *Peridinium limbatum* (A.Stokes) Lemmerm. (100LBS, 1.00BPP), *Peridinium bipes* F.Stein (87LBS, 0.98BPP) and the *P. willei* species group (100LBS, 1.00BPP). The latter was composed of two lineages including accessions either assigned to *P. willei* (81LBS) or to *P. volzii* (98LBS, 1.00BPP). Based on ITS sequences data three maximally supported ribotypes were distinguished within *P. volzii*, in which SSU and/or LSU sequences gained from the strains NIES501 and PWCL1 were likewise included. No compensatory base substitutions or altered secondary

**Table 1** Size of motile and coccoid cells, length of specific sutures and frequency of morphological characteristics including thecal opening of seven selected strains

	GeoM*793	GeoM*788	GeoM*789	GeoM*866	GeoK*024	GeoK*037	GeoK*044	
Ribotype	I	II	II	III	III	III	III	
Motile cell length	40.96	46.15	45.80	49.57	50.96	50.69	50.74	<i>n</i> = 50
Motile cell width	36.09	41.92	41.18	47.06	48.14	47.79	46.93	<i>n</i> = 50
Ratio motile cell length and width	1.13	1.10	1.11	1.05	1.06	1.07	1.08	<i>n</i> = 50
Cocoid cell length	39.11	43.86	45.84	43.41	44.96	50.68	45.04	<i>n</i> = 50
Cocoid cell width	32.64	38.53	38.97	36.54	42.65	45.19	42.08	<i>n</i> = 50
Suture length 1'≡2'	6.88	7.48	7.12	7.38	7.26	7.40	7.42	<i>n</i> = 50
Suture length 1'≡4'	10.30	10.20	10.64	12.86	12.00	12.37	12.52	<i>n</i> = 50
Cingulum displacement 1 ×	100%	88%	74%	4%	2%	2%	6%	<i>n</i> = 100
Cingulum displacement 1.5 ×–2 ×	0%	12%	26%	96%	98%	98%	94%	<i>n</i> = 100
Cell division line regular	82%	79%	74%	66%	81%	81%	80%	<i>n</i> = 100
Antapical plates of unequal size	88%	92%	90%	78%	92%	90%	74%	<i>n</i> = 100

structures were identified among the ITS ribotypes assigned to *P. volzii*.

## Discussion

### *Peridinium volzii* is morphologically distinct from *Peridinium willei*

Correct and consistent species identification is the necessary prerequisite for investigations of ecosystem dynamics

and conservation strategies. However, delimitation and determination of unicellular organisms at the species level are challenging due to complex identification procedures. Exemplarily, there has been some uncertainty whether the names, *P. volzii* and *P. willei* represent a single species (Playfair, 1920; Popovský & Pfister, 1990) or in fact two distinct species. The integrative approach followed in this study, combining a molecular phylogenetic tree and detailed morphological investigations, unequivocally shows the distinctiveness of the two entities and their sister group relationship. The differences in the ecological

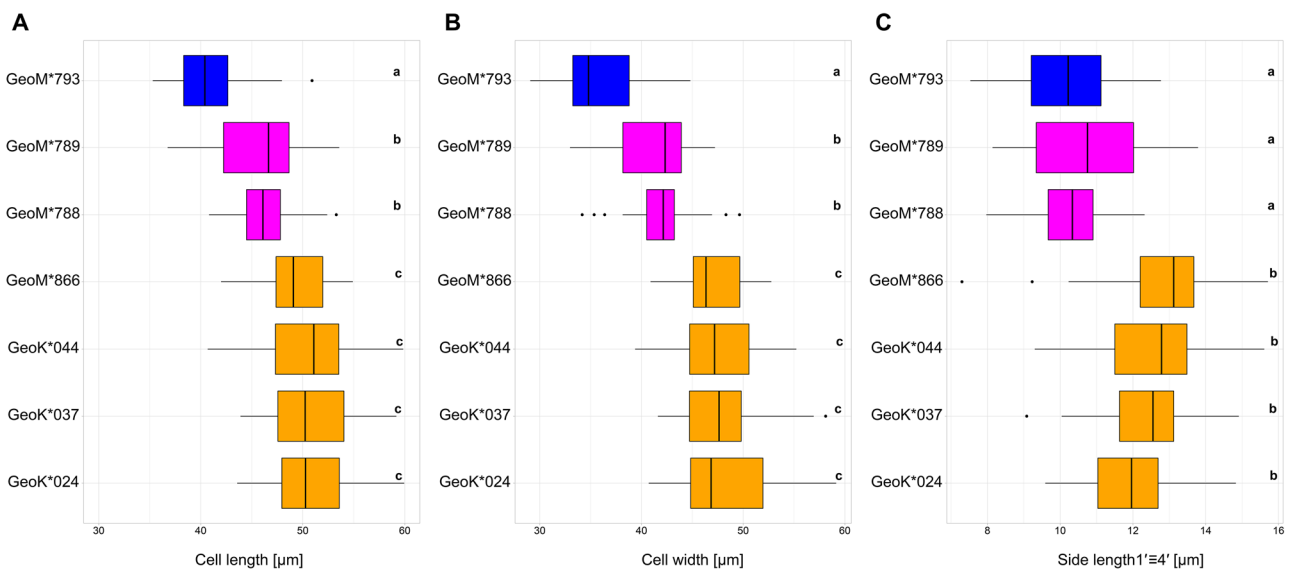


**Fig. 2** Box plots displaying correlations between cell size (of motile cells; **A**, **B**) or side length (of empty thecae cells; **C**) in selected strains. Colours correspond to the ribotype of each strain (blue: ribotype I; magenta: ribotype II; orange: ribotype III). Statistically significant clusters are indicated with letters **a**, **b** and

**c** and were calculated with Tukey's Honest Significant Difference (HSD) test (*p*-values < 0.05). Box plots depict percentile values from 25–75% (box), median (bar inside the box), standard deviation (whiskers) and outliers (dots)

**Table 2** Basionyms that have been associated with *P. volzii*, with diagnostic traits and further information as inferred from the protologues, and abundance of such traits in the investigated material

Basionym, protologue	Diagnostic trait(s)	Length/width [ $\mu\text{m}$ ]	Cingulum displacement	Ribotype (frequency) [ $n=100$ for each ribotype]	Image
<i>P. tabularum</i> var. <i>maeandricum</i> Lauterborn, <i>nom. corr.</i> (ICN Art. 23.5), Verhandlungen des Naturhistorisch-Medicinischen Vereins zu Heidelberg n.s. 7: 604 (1904)	Meandering ridges on plates' surface	62–70/68–74	–	I (–), II (–), III (–)	Hansen & Flaim (2007: Fig. 16A, G)
<i>P. volzii</i> Lemmerm., Abhandlungen herausgegeben vom Naturwissenschaftlichen Verein zu Bremen 18: 166–167, pl. XI 15–18 (1905)	Plate 1' small	38/–	1 X	I (100%), II (100%), III (100%)	1a–i
<i>P. volzii</i> var. <i>australe</i> G.S. West, Journal of the Linnean Society. Botany 39: [12, 19, 32, 41, 45,]80[–81], Fig. 10A–G (1909)	Plates 1''' and 2''' of unequal size	40–56/39–59	1.5 X	I (86%), II (90%), III (83.5%)	3i
<i>P. volzii</i> var. <i>maximum</i> C. Bernard, Sur quelques algues unicellulaires: 82, Fig. 186 (1909)	Larger cell size	47–58/47–54	–	I (1%), II (4%), III (45%)	–
<i>P. gvestrowiense</i> Er.Lindem., Archiv für Hydrobiologie und Planktonkunde 11: 490–491, Figs 1–3 (1916)	Unawareness of <i>P. volzii</i> , but without antapical spine	42–48/42–48	1 X	I (100%), II (100%), III (100%)	–
<i>P. gvestrowiense</i> forma <i>late-intercalatum</i> Er.Lindem., Archiv für Hydrobiologie und Planktonkunde 11: 491–492, Figs 4–5 (1916)	Broad sutures	38–44	1 X	I, II, III (broad range)	1a; 3b, i
<i>P. gvestrowiense</i> forma <i>latissime-intercalatum</i> Er.Lindem., Archiv für Hydrobiologie und Planktonkunde 11: 492, Figs 9–10 (1916)	Even broader sutures	38–44	–	I, II, III (broad range)	3e, k–l
<i>P. gvestrowiense</i> forma <i>geniculatum</i> Er.Lindem., Deutsche Gesellschaft für Kunst und Wissenschaft in Posen. Zeitschrift der Naturwissenschaftlichen Abteilung (des Naturwissenschaftlichen Vereins). Posen 25: 25 (1918)	Obtuse angle between plates 2' and 4'	–	–	I (–), II (–), III (–)	–
<i>P. gvestrowiense</i> forma <i>lineatum</i> Er.Lindem., Deutsche Gesellschaft für Kunst und Wissenschaft in Posen. Zeitschrift der Naturwissenschaftlichen Abteilung (des Naturwissenschaftlichen Vereins). Posen 25: 25 (1918)	Plates 1a, 2a, 3' narrow	–	–	I (1%), II (1%), III (1%)	3g
<i>P. gvestrowiense</i> forma <i>sinuatum</i> Er.Lindem., Archiv für Protistenkunde 39: 248–249, Figs 107–110 (1919)	Transversal bending	–	0.5 X	I (1%), II (1%), III (1%)	–
<i>P. gvestrowiense</i> forma <i>compressum</i> Er.Lindem., Archiv für Protistenkunde 39: 249, Figs 111–113 (1919)	Dorso-ventral compression	42/–	1 X	I (1%), II (1%), III (1%)	3h
<i>P. gvestrowiense</i> forma <i>cyclicum</i> Er.Lindem., Archiv für Naturgeschichte 84.8: 156, Figs 123–124 (1920)	Cyclic configuration of apical plates	46/–	1.5 X	I (1%), II (1%), III (1%)	–
<i>P. gvestrowiense</i> subvar. <i>originale</i> Er.Lindem., Archiv für Naturgeschichte 84.8: 158, Fig. 133 (1920)	Plate 3''' split	–	–	I (1%), II (2%), III (1%)	3i
<i>P. gvestrowiense</i> var. <i>betacollineatum</i> Er.Lindem., Archiv für Naturgeschichte 84.8: 179, Fig. 190 (1920)	$\beta$ -collineation between plates 3a 4', 5'', 6''	–	–	I (–), II (–), III (–)	–
<i>P. willetii</i> var. <i>botanicum</i> Playfair, Proceedings of the Linnean Society of New South Wales 44: 813, pl. XLI 3 (1920)	Two posterior spines, plates 1''' and 2''' of equal size	42–60/40–60	2	I (–), II (–), III (–)	–



Table 2 (continued)

Basionym, protologue	Diagnostic trait(s)	Length/width [ $\mu\text{m}$ ]	Cingulum displacement	Ribotype (frequency) [ $n=100$ for each ribotype]	Image
<i>P. volzii</i> var. <i>cinctiforme</i> M.Lefèvre, Bulletin du Museum d'Histoire Naturelle. Paris 33: 122 (1927)	Plates 2' and 4' very unequal in size	–	–	I (26%), II (29.5%), III (41.5%)	3k
<i>P. volzii</i> var. <i>simplex</i> M.Lefèvre, <i>stat. corr.</i> (ICN Art. 24.4.), Bulletin du Museum d'Histoire Naturelle. Paris 33: 122 (1927)	Plates 1''' and 2''' fused	–	–	I (5%), II (2%), III (1%)	3l
<i>P. playfairii</i> Er.Lindem., Archiv für Hydrobiologie 8 Suppl.: 715–716, Figs 43–44 (1931)	APC present	40–50/–	1.5×	I (–), II (–), III (–)	–
<i>P. vanconverense</i> Wailes, <i>nom. nov. pro P. striolatum</i> Wailes, Annales de Protistologie 3: 110 (1931)	Ornamentation with linear ridges	52–60/55–60	0.5×	I (–), II (–), III (–)	–
<i>P. volzii</i> forma <i>complexum</i> Krakhamalny in Krakhamalny, Wasser, Nevo, Boltovskoy, Barinova & Krakhamalny, International Journal of Algae 6: 214, Fig. 2, pl. II 3–6 (2004)	Plate 3' split	35–50/25–45	1.5×	I (1%), II (1%), III (1%)	3m

preferences in the two species provide further evidence for their separation (Höll, 1928; Olrek, 1992).

Bachmann (1911) was probably the first to accept two distinct species. In addition to *P. willei*, also Lindemann (1918) recognised a second species, initially his *P. gues-trowiense* (Lindemann, 1916) and since Lindemann (1924) at the latest the older *P. volzii*. The most striking diagnostic trait is the size of the first apical plate, which is large in the lineage including accessions determined as *P. willei* and which is small in the lineage including those determined as *P. volzii*. Only strain PWCL1 has been determined as *P. willei* (Logares et al., 2007) but is placed on the branch of *P. volzii*. However, no morphology is known from this strain, and it is likely a misidentification. Ling et al. (1989) reported from intermediates between *P. volzii* and *P. willei* but in the strains studied here in detail, the first apical plate was always small, without exception. From a phylogenetic perspective, the character state is presumably apomorphic for *P. volzii* (versus bigger in other Peridiniaceae including *P. willei* as ancestral state).

### *Peridinium volzii* is morphologically variable

Despite the uniqueness of *P. volzii* due to the small first apical plate, the morphological plasticity within the evolutionary lineage appears great. However, all this plasticity (shown within monoclonal strains and partly formalised in numerous varieties and forms) cannot be associated with other traits such as environmental conditions, geographic occurrence or genetic constitution that evolutionary adaptation appears of minor importance in *P. volzii*. A considerable number of infraspecific taxa have been described (Table 2) and based on the microscopic study of monoclonal strains we confirm the existence of traits such as additional sutures (associated with, e.g., *P. volzii* forma *complexum*; Fig. 3m) and fusion of plates (associated with, e.g., *P. volzii* var. *simplex*; Fig. 3l). Other traits such as the shifted suture (of *Peridinium gues-trowiense* var. *betacollineatum* Er.Lindem.) having importance in species such as *P. cinctum* (Izquierdo López et al., 2018; Romeikat et al., 2019) have not been found during the course of the present study. It is known today that varying widths of sutures, where the intercalary space becomes distinctively striate, are ontogenetically disposed (growth bands: Netzel, 1982). This trait (Figs. 1a, 3b, e, i, k) is associated with *P. gues-trowiense* forma *late-intercalatum* and *P. gues-trowiense* forma *latissime-intercalatum* Er.Lindem. and is the only one that occurs in combination with other morphological deviations.

The diagnostic trait of *P. volzii* var. *australe* G.S.West is the antapical plates of unequal size (versus equal size in *P. volzii* var. *volzii*), and this character state is frequent (> 70%) in the material under investigation (Fig. 3i). Similarly, the diagnostic trait of *P. volzii* var. *cinctiforme* M.Lefèvre is the apical plates



**Table 3** Newly identified phenotypical variabilities in strains determined as *P. volzii*. Frequency determined for each ribotype ( $n = 100$ )

Variation	Ribotype	Image
Plate 4'' pentagonal	I (21%), II (3%), III (1%)	$n = 100$ for each ribotype 3b
Plate 2a split	I (3%), II (2%), III (3%)	$n = 100$ for each ribotype 3c
Plates 1a and 3' fused	I (7%), II (6%), III (2%)	$n = 100$ for each ribotype 3f
Plates 2'' and 3'' fused	I (2%), II (1%), III (1%)	$n = 100$ for each ribotype 3d
Plates 1''' and 1'''' fused	I (1%), II (1%), III (1%)	$n = 100$ for each ribotype 3e

2' and 4' of unequal size (versus rather equal size in *P. volzii* var. *volzii*), and this character state (distinctive in species such as *P. cinctum* and *Peridinium raciborskii* Wołosz.) is also not rare (25–50%) in the material studied here (Fig. 3k). We even confirm the existence of *Peridinium guestrowiense* subvar. *originale* Er.Lindem. having six postcingular plates (versus five such plates usually present in peridiniacean dinophytes; Fig. 3i). The reduction from six to five postcingular plates in Peridinales may result from a fusion of the third and fourth postcingular plate (Gottschling et al., 2021) present today in dinophytes such as the Amphidomataceae (Tillmann et al., 2009). Already Lindemann (1920: 122) pointed out the possibility that phylogenetically ancestral character states occasionally recur (known as atavism), which is corroborated by our observations of individual such cells in monoclonal strains. However, all such variation occurs in individual cells and cannot be associated with other traits such as a genetic constitution or geographic occurrence. Therefore, the recognition of corresponding taxa at infraspecific ranks does not appear justified.

In addition to the historically described intraspecific variabilities, we detected five cases of yet undiscovered deviation in *P. volzii*. The unusual epithelial configuration with plate 4'' abutting plate 3a (Fig. 3a-b) has to the best of knowledge never been noted in the literature before. More-over, alternate configurations between, for example, plates 3' and 4'' (resp. 1a and 3a; Fig. 1c, f) within monoclonal strains are reminiscent of, for example, *Parvodinium mixtum* Wołosz. ex Kretschmann, Zerdoner, Owsianny & Gottschling (Kretschmann et al., 2018a). An additional suture and the split of plate 2a (Fig. 3c) have also not been reported from *P. volzii* so far. Fusion of plates regularly though rarely appears in the thecal pattern of various dinophytes, and corresponding observations in the present study do not come as a surprise. Usually, the fusion of plates takes place within plate series such as the intercalary (Fig. 3f), precingular (Fig. 3d) and antapical series (associated with *P. volzii* var. *simplex*; Fig. 3l). However, the fusion of plates associated with different plate series is very rare, and we found fused plates 1''' and 1'''' (Fig. 3e) once only. Anyhow, also the newly discovered variability occurs in individual cells associated with all three ribotypes present in this study and does not make the recognition of corresponding taxa at an infraspecific rank seem justified either.

## Correlations between ribotypes and morphotypes

The goal and importance of Linnaean binomials in nomenclature is to avoid different scientific names for the same biological entity (Minelli, 2019). Phenotypic variants occur at several interindividual levels, such as between reproductively isolated units (i.e., species), between populations (e.g., local communities) or within populations (e.g., alleles). There is no ultimate consensus about the usefulness of infraspecific taxonomic ranks (such as subspecies, varieties and forms) in order to provide such variants with scientific names. In practice, different taxonomists (at different points in time) treat(ed) phenotypic variation differently (Knapp et al., 2004; Mayr, 1982a, b) and created considerable complexity (Hamilton & Reichard, 1992), also in dinophytes (Izquierdo López et al., 2018; Moestrup & Calado, 2018; Romeikat et al., 2019). Intraspecific classifications should only be made with a certain reserve, as categorisation of minor morphological variability conflicts with the practical goal of stability in taxonomy (Boenigk et al., 2012; Turland, 2019; Warburton, 1967). As criteria for the acceptance of taxonomic entities, the present case studies possible correlations between genetic disposition (i.e., certain ribotypes), morphology (i.e., diagnostic traits) and/or geographic occurrence. There is considerable variation (previously already observed based on enzyme electrophoresis and flow cytometric determination of nuclear DNA quantities: Hayhome et al., 1987), and the basic question is whether the evolutionary lineage of *P. volzii* as displayed in the molecular tree represents a single or several species. In the previous part of the discussion, we have already argued that most of the infraspecific taxa described so far are not suitable as taxonomic subsets of *P. volzii*.

No morphological and ITS sequence information is available for strains PWCL1 and NIES501, that they are not worthy to be considered further here. However, there are significant correlations to the state between certain ITS ribotypes and the three traits cell size, cingulum displacement and length of the suture between plates 1' and 4', respectively. Data overlap is very low, which underlines the distinctiveness of certain character states. Ribotype I is associated with the smallest cell size, the single-width displacement of the cingulum and a short suture. Morphometrics are similar for ribotype II, which shows, however, greater cell size. Ribotype III is

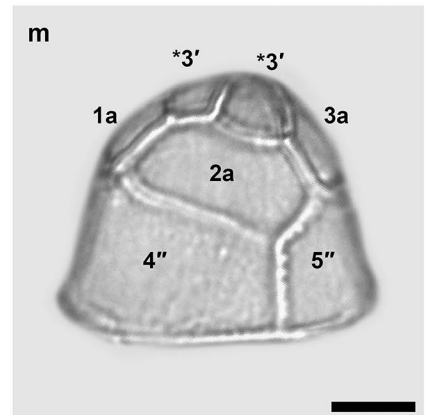
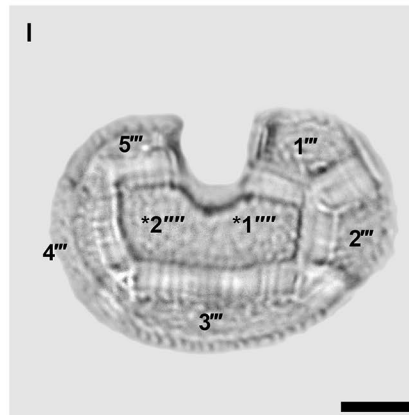
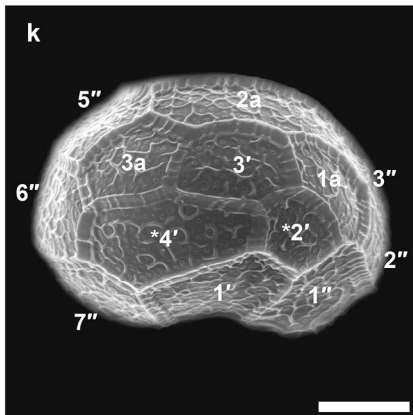
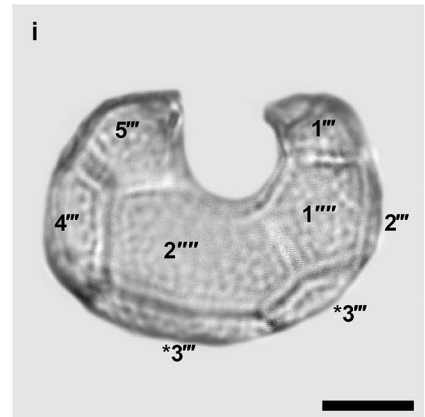
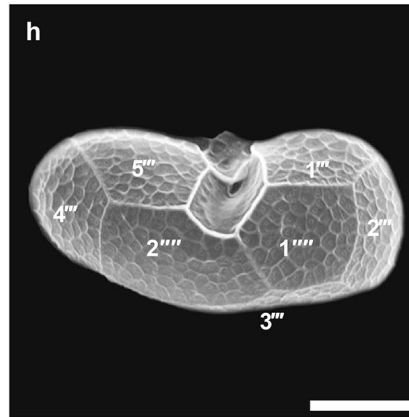
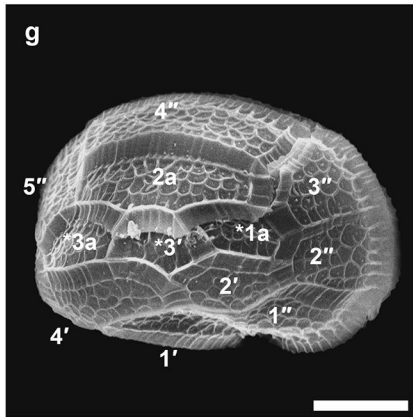
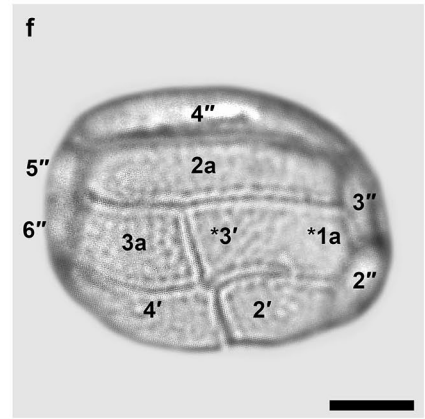
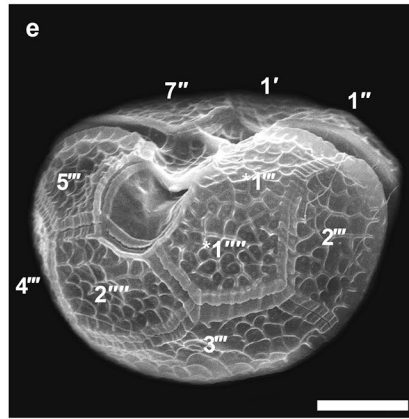
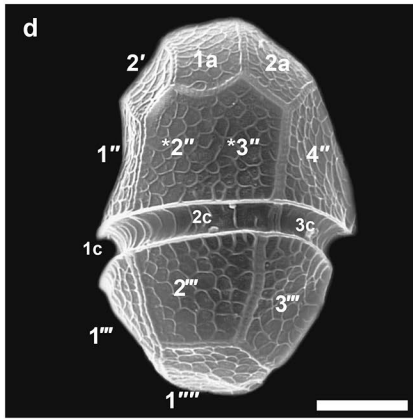
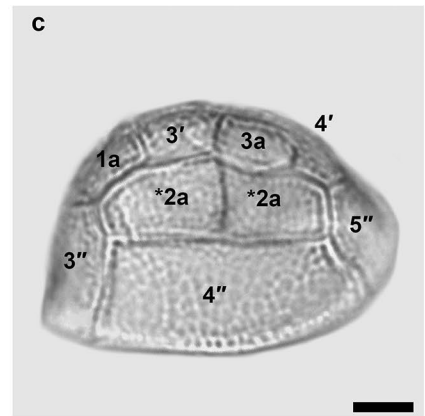
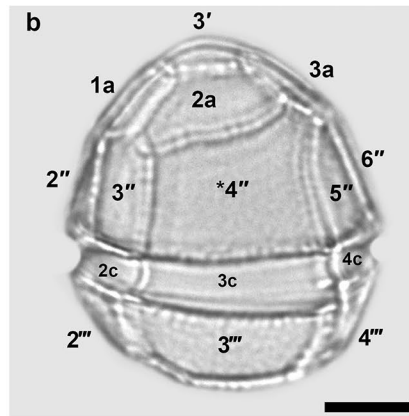
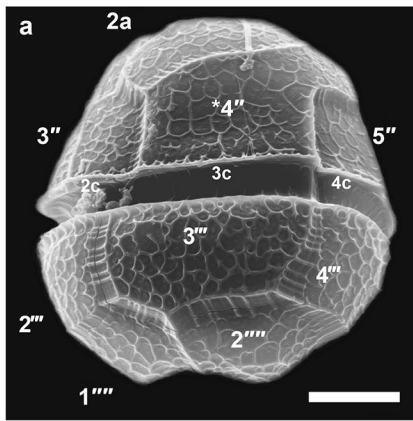


**Fig. 3** Historically described phenotypical variations and yet undiscovered deviations in the plate pattern of *P. volzii*. **b–c, f, i, l–m** Light microscopy, **a, d–e, g–h, k** scanning electron microscopy. **a–f** Newly identified deviations **a–b** plate 4'' pentagonal in strains **a** GeoM\*793; **b** GeoM\*788; **c** plate 2a split (strain GeoK\*024); **d** plates 2'' and 3'' fused (strain GeoM\*866); **e** plates 1''' and 1'''' fused (strain GeoM\*788); **f** plates 1a and 3' fused (strain GeoM\*788). **g–m** Historic infraspecific taxa; **g** *P. guestrowiense* forma *lineatum* (strain GeoM\*866); **h** *P. guestrowiense* forma *compressum* (strain GeoM\*866); **i** *P. guestrowiense* subvar. *originale* (strain GeoK\*024); **k** *P. volzii* var. *cinctiforme* (strain GeoM\*793); **l** *P. volzii* var. *simplex* (strain GeoM\*789); **m** *P. volzii* forma *complexum* (strain GeoM\*793). Abbreviations: n': apical plate, n'': precingular plate, n''': postcingular plate, n''': antapical plate, na: anterior intercalary plate, nC: cingular plate, split or fused plates are indicated by asterisks. Scale bar = 10 µm.  $U_A = 15$  kV

distinct by the combination of the greatest cell size, a displacement of the cingulum beyond 1.5 fold the width and a long suture. Notably, the similarity between cells assigned to ribotypes I and II is greater than any of them to ribotype III, but ribotypes II and III are closely related in the DNA tree. However, no unequivocal or operable correlations between certain ribotypes, diagnostic traits, ecological preferences and/or geographic occurrence can be drawn. Cryptic speciation (Fenchel, 2005) can certainly not be excluded as it has been shown for other dinophytes (Lajeunesse et al., 2012; Luo et al., 2017; Montresor et al., 2003; Wang et al., 2019), but a single, variable species *P. volzii* is more likely at this moment in time, as it was worked out also for *P. cinctum* of the same phylogenetic group (Izquierdo López et al., 2018).

### Life-history

Life-history and metagenesis of Peridiniaceae is complex and not fully understood at present. Sexual reproduction of *P. volzii* is isogamous and heterothallic and includes motile and coccoid cells during the diploid stage (Hayhome et al., 1987; Kita & Fukuyo, 1995; Pfiester & Skvarla, 1979). In our monoclonal strains, we have never observed any fusion of cells (with subsequent karyogamy) or four-cell aggregations (i.e., indication for meiosis). This confirms observations of Pfiester and Skvarla (1979) that sexuality does not take place within monoclonal strains of *P. volzii* (other Peridiniaceae are homothallic: Pfiester, 1975, 1976, 1977). Three size classes are stated for the motile cells of *P. volzii* (Pfiester & Skvarla, 1979) and other Peridiniaceae (Pfiester, 1975, 1976, 1977), namely small cells < 30 µm (gametes, certainly haploid), large cells ≥ 60 µm (zygotes, certainly diploid) and mid-sized cells, which are in the range described in the present study. The ploidy level of these motile cells is unknown at present, but it is not improbable that they are haploid as the gametes. Subsequently, the various coccoid cells observed in the present study are all most likely also part of the haploid stage (as

sexuality does not take place within monoclonal strains). The here reported, intrathecatly formed coccoid cells are morphologically not differentiated from the coccoid cells of the diploid stage. Pfiester and Skvarla (1979) do not provide exact measurements for those cells they term hypnozygotes, but they are probably bigger than the otherwise indistinguishable cells in our study. More research is necessary to entangle all these different cell types and place them properly in the metagenesis of Peridiniaceae.

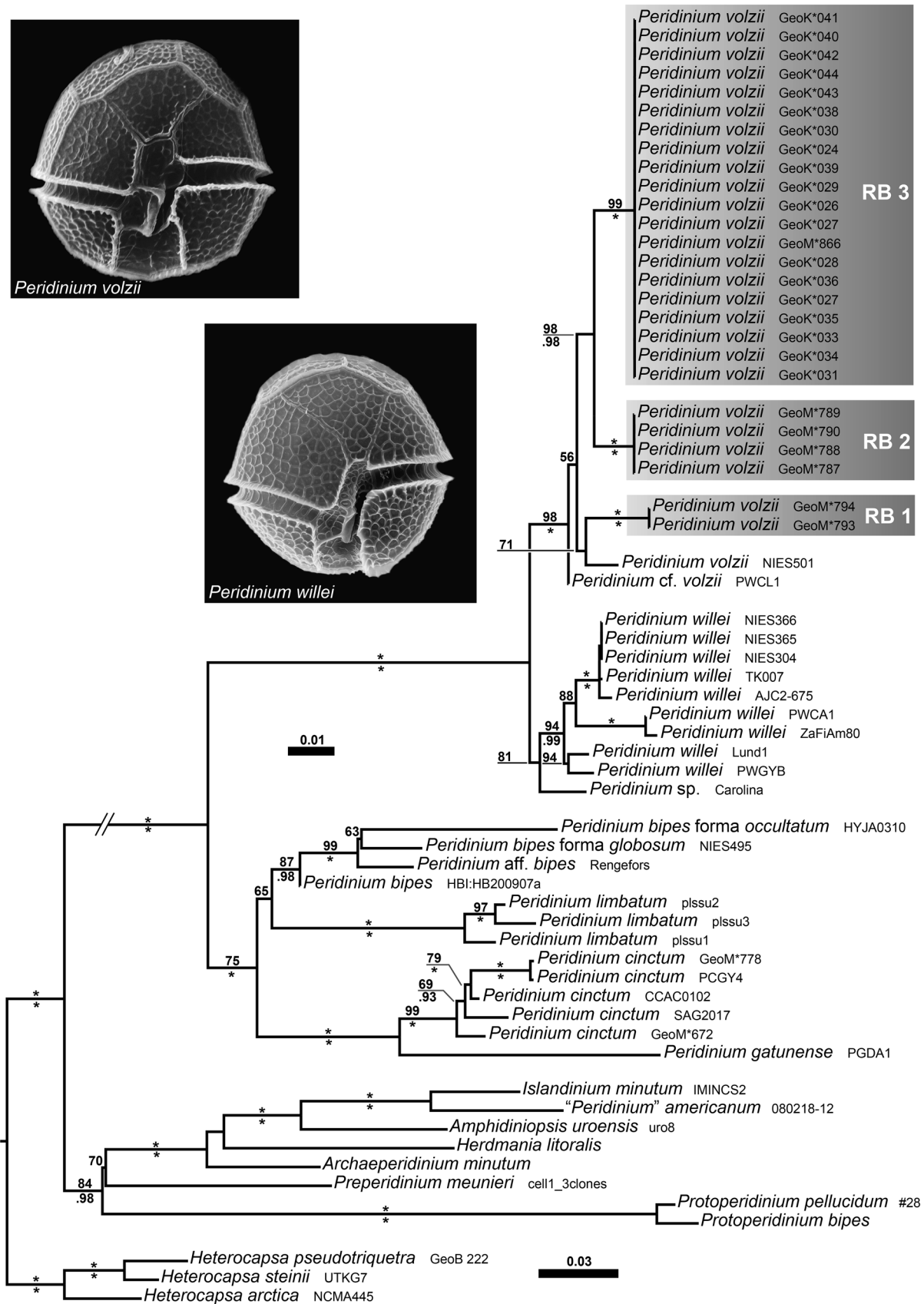
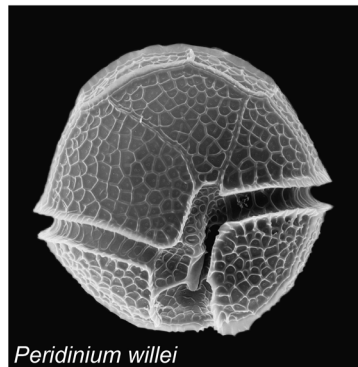
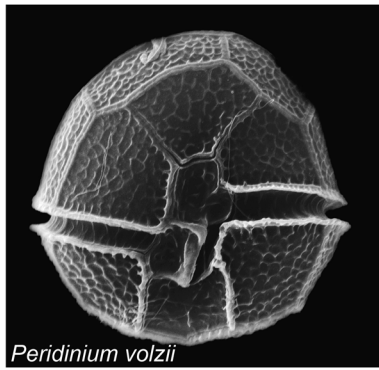
Little attention has been put in the past on the dissociation of thecal elements during mitotic cell division. For the closely related *P. willei*, Moestrup and Calado (2018) state that the epitheca segregates into pieces, one of which is said to be composed of the plates 2', 1a–3a, 3'''–5'''. In *P. volzii*, the lid is composed of the plates 3', 1a–3a, 3'''–5'', and whether the break of the epitheca is truly different between the two species, or whether the information provided by Moestrup and Calado (2018) contain typos, remains to be determined (no reference provided). The opening of the cells during regular mitosis has not been observed in *P. limbatum*, but the dehiscence line on the epitheca during the formation of the coccoid cell (Evvit & Wall, 1968; Wall & Dale, 1968) is similar to *P. volzii*. However, the hypotheca remains entire in the latter species, whereas it also splits in *P. limbatum* during the release of the coccoid cell. Notably, the course of the archaeopyle of *P. limbatum* is identical to the observations made for the epitheca of *P. volzii*. Alternative sheds of the theca, such as the dorso-ventral split of the epitheca in †*Lingulodinium* D.Wall (Tillmann et al., 2021) or the hypotheca opening in Peridiniopsidaceae (Kretschmann et al., 2018a), may indicate that this trait is phylogenetically informative, but not sufficiently investigated so far.

### Conclusion

The integrative approach presented here studying both morphological and molecular data is important to clarify the boundaries between species in the microbial domain. Based on monoclonal strains established from recently collected material we confirmed a great morphological and genetic variability in *P. volzii*. However, the decision whether the three ITS ribotypes correspond to one, two or three species is impossible to make the present data given. Morphological data of strains NIES501 from Japan and PWCL1 from Wisconsin, or published molecular data of strain SCCAP K-1155 from Italy (Hansen & Flaim, 2007), would probably render a clearer structure to delimit species and populations within dinophytes such as *P. volzii*.

In the light of the present new data, it is worthy to reconsider the taxonomic status of scientific names associated with *P. volzii*, but also of the species itself described





Peridiniaceae

PPE

HET



**Fig. 4** A molecular tree of 51 systematically representative Peridiniaceae, including all 28 accessions assignable to *P. volzii*. Maximum Likelihood tree ( $-\ln = 22,017.62$ ), as inferred from a rRNA nucleotide alignment (1,129 parsimony-informative sites) and with strain number information. Numbers on branches are ML bootstrap (above) and Bayesian support values (below) for the clusters (asterisks indicate maximal support values, values under 50 and 0.90, respectively, are not shown). Clades are indicated (abbreviations: HET, Heterocapsaceae; PPE, Protoperidiniaceae)

from Singapore. In the protologue, Lemmermann (1905) highlighted the trait of an antapical spine, which appears abundant in material from Singapore, Indonesia and Australia (Lindemann, 1931; Ling et al., 1989; Playfair, 1920; West, 1909). Such spine is absent from all illustrations we are aware of from Central Europe (Baumeister, 1976; Entz, 1927; Lefèvre, 1932; Lewis & Dodge, 2011; Lindemann, 1916, 1920; Olrik, 1992; Крахмальный, 2011), and it is also absent without exception from the material studied here. Cells from Australasia are also remarkably smaller than those reported from Europe. Doubts are allowed that true *P. volzii* occurs in Central Europe at all, and future studies must clarify the distinctiveness from German *P. guestrowiense* as next-younger scientific name. Similarly, *P. volzii* var. *maeandricum* has a very distinctive ornamentation, of which it is said being consistent within strains (Hansen & Flaim, 2007). This could be indicative for the species status of *Peridinium maeandricum* (Lauterborn) V.Brehm rather than for the variety level, and the characteristic ornamentation is consistently absent from the material studied here. More research is necessary to entangle the complex interactions between genetic disposition, morphological variation and geographic occurrence of unicellular organisms such as *P. volzii* and its relatives.

**Supplementary Information** The online version contains supplementary material available at <https://doi.org/10.1007/s13127-021-00514-y>.

**Acknowledgements** We sincerely thank Eva Facher (Munich) for assistance in the lab.

**Funding** Open Access funding enabled and organized by Projekt DEAL. This work was supported by the Deutsche Forschungsgemeinschaft (grant GO1459 10–1).

**Data availability** The datasets generated during and analysed during the current study will be available in the GenBank repository after acceptance of the manuscript. The corresponding Accession numbers are listed in the Voucher List (Table S1). Comprehensive morphological data are available from the corresponding author on reasonable request.

**Open Access** This article is licensed under a Creative Commons Attribution 4.0 International License, which permits use, sharing, adaptation, distribution and reproduction in any medium or format, as long as you give appropriate credit to the original author(s) and the source, provide a link to the Creative Commons licence, and indicate if changes

were made. The images or other third party material in this article are included in the article's Creative Commons licence, unless indicated otherwise in a credit line to the material. If material is not included in the article's Creative Commons licence and your intended use is not permitted by statutory regulation or exceeds the permitted use, you will need to obtain permission directly from the copyright holder. To view a copy of this licence, visit <http://creativecommons.org/licenses/by/4.0/>.

## References

- Altschul, S. F., Gish, W., Miller, W., Myers, E. W., & Lipman, D. J. (1990). Basic local alignment search tool. *Journal of Molecular Biology*, 215, 403–410.
- Bachmann, H. (1911). *Das Plankton des Süßwassers mit besonderer Berücksichtigung des Vierwaldstättersees*. Jena: Fischer.
- Baumeister, W. (1976). Über die Artbestimmung der großen Cleisto- und Poroperidineen unserer Gewässer. *Arbeitsstätte Zur Erforschung Des Lebens in Kleingewässern, Mitteilungen*, 9, 1–6.
- Blackburn, S. I., Bolch, C. J. S., Haskard, K. A., & Hallegraeff, G. M. (2001). Reproductive compatibility among four global populations of the toxic dinoflagellate *Gymnodinium catenatum* (Dinophyceae). *Phycologia*, 40, 78–87.
- Blaxter, M. L. (2004). The promise of a DNA taxonomy. *Philosophical Transactions of the Royal Society of London Series B-Biological Sciences*, 359, 669–679.
- Boenigk, J., Ereshefsky, M., Hoef-Emden, K., Mallet, J., & Bass, D. (2012). Concepts in protistology: Species definitions and boundaries. *European Journal of Protistology*, 48, 96–102.
- Camargo, J. A. (1994). The importance of biological monitoring for the ecological risk assessment of freshwater pollution: A case study. *Environment International*, 20, 229–238.
- Chevin, L.-M., Lande, R., & Mace, G. M. (2010). Adaptation, plasticity, and extinction in a changing environment: Towards a predictive theory. *PLoS Biology*, 8, 1000357.
- De Clerck, O., Guiry, M. D., Leliaert, F., Samyn, Y., & Verbruggen, H. (2013). Algal taxonomy: A road to nowhere? *Journal of Phycology*, 49, 215–225.
- Entz, G. (1927). A Balaton peridineáiról. Über Peridineen des Balaton-Sees. *Archivum Balatonicum*, 1, 275–342.
- Evitt, W. R., & Wall, D. (1968). Dinoflagellate studies IV. Thecae and cyst of recent freshwater *Peridinium limbatum* (Stokes) Lemmermann. *Stanford University Publications. Geological Sciences*, 12, 1–15.
- Fenchel, T. (2005). Cosmopolitan microbes and their “cryptic” species. *Aquatic Microbial Ecology*, 41, 49–54.
- Figueroa, R. I., Rengefors, K., Bravo, I., & Bensch, S. (2010). From homothally to heterothally: Mating preferences and genetic variation within clones of the dinoflagellate *Gymnodinium catenatum*. *Deep-Sea Research Part II-Topical Studies in Oceanography*, 57, 190–198.
- Gottschling, M., Carbonell-Moore, M. C., Mertens, K. N., Kirsch, M., Elbrächter, M., & Tillmann, U. (2021). *Fensomea setacea*, gen. & sp. nov. (Cladopyxidaceae, Dinophyceae), is neither gonyaulacoid nor peridinioid as inferred from morphological and molecular data. *Scientific Reports*, 11, 12824.
- Gottschling, M., Chacón, J., Žerdoner Čalasan, A., Neuhaus, S., Kretschmann, J., Stibor, H., et al. (2020). Phylogenetic placement of environmental sequences using taxonomically reliable databases helps to rigorously assess dinophyte biodiversity in Bavarian lakes (Germany). *Freshwater Biology*, 65, 193–208.
- Gottschling, M., & Plötner, J. (2004). Secondary structure models of the nuclear Internal Transcribed Spacer regions and 5.8S rRNA in Calciodinelloideae (Peridiniaceae) and other dinoflagellates. *Nucleic Acids Research*, 32, 307–315.
- Gottschling, M., Söhner, S., Zinßmeister, C., John, U., Plötner, J., Schweikert, M., et al. (2012). Delimitation of the

- Thoracosphaeraceae (Dinophyceae), including the calcareous dinoflagellates, based on large amounts of ribosomal RNA sequence data. *Protist*, 163, 15–24.
- Guillard, R. R., & Lorenzen, C. J. (1972). Yellow-green algae with chlorophyllide c. *Journal of Phycology*, 8, 10–14.
- Hamilton, C. W., & Reichard, S. H. (1992). Current practice in the use of subspecies, variety, and forma in the classification of wild plants. *Taxon*, 41, 485–498.
- Hansen, G., & Flaim, G. (2007). Dinoflagellates of the Trentino Province, Italy. *Journal of Limnology*, 66, 107–141.
- Hayhome, B. A., & Pfister, L. A. (1983). Electrophoretic analysis of soluble enzymes in five freshwater dinoflagellate species. *American Journal of Botany*, 70, 1165–1172.
- Hayhome, B. A., Whitten, D., Harkins, K., & Pfister, L. A. (1987). Intraspecific variation in the dinoflagellate *Peridinium volzii*. *Journal of Phycology*, 23, 573–580.
- Hellawell, J. M. (1986). *Biological indicators of freshwater pollution and environmental management (Pollution Monitoring Series)*. London: Elsevier.
- Höll, K. (1928). *Oekologie der Peridineen. Studien über den Einfluß chemischer und physikalischer Faktoren auf die Verbreitung der Dinoflagellaten im Süßwasser* (Pflanzenforschung 11). Jena: Fischer.
- Izquierdo López, A., Kretschmann, J., Žerdoner Čalasan, A., & Gottschling, M. (2018). The many faces of *Peridinium cinctum*: Morphological and molecular variability in a common dinophyte. *European Journal of Phycology*, 53, 156–165.
- Janofske, D. (2000). *Scrippsiella trochoidea* and *Scrippsiella regalis*, nov. comb. (Peridinales, Dinophyceae): A comparison. *Journal of Phycology*, 36, 178–189.
- Katoh, K., & Standley, D. M. (2013). MAFFT multiple sequence alignment software version 7: Improvements in performance and usability. *Molecular Biology and Evolution*, 30, 772–780.
- Keck, F., Vasselon, V., Rimet, F., Bouchez, A., & Kahlert, M. (2018). Boosting DNA metabarcoding for biomonitoring with phylogenetic estimation of operational taxonomic units' ecological profiles. *Molecular Ecology Resources*, 18, 1299–1309.
- Ki, J.-S., Park, M.-H., & Han, M.-S. (2011). Discriminative power of nuclear rDNA sequences for the DNA taxonomy of the dinoflagellate genus *Peridinium* (Dinophyceae). *Journal of Phycology*, 47, 426–435.
- Kita, T., & Fukuyo, Y. (1995). Life history of *Peridinium volzii* (Dinophyceae) in a natural pond. *Bulletin of the Plankton Society of Japan*, 42, 63–73.
- Knapp, S., Lamas, G., Lughadha, E. N., & Novarino, G. (2004). Stability or stasis in the names of organisms: The evolving codes of nomenclature. *Philosophical Transactions of the Royal Society B-Biological Sciences*, 359, 611–622.
- Крахмальний, А. Ф. (2011). *Динофитовые водоросли Украины (иллюстрированный определитель)*. Киев: Альтерпрес.
- Kremp, A., Tahvanainen, P., Litaker, W., Krock, B., Suikkanen, S., Leaw, C. P., & Tomas, C. (2014). Phylogenetic relationships, morphological variation, and toxin pattern in the *Alexandrium ostenfeldii* (Dinophyceae) complex: Implications for species boundaries and identities. *Journal of Phycology*, 50, 81–100.
- Kretschmann, J., Owsiany, P. M., Žerdoner Čalasan, A., & Gottschling, M. (2018a). The hot spot in a cold environment: Puzzling *Parvodinium* (Peridiniopsidaceae, Peridinales) from the Polish Tatra Mountains. *Protist*, 169, 206–230.
- Kretschmann, J., Žerdoner Čalasan, A., & Gottschling, M. (2018b). Molecular phylogenetics of dinophytes harbouring diatoms as endosymbionts (Kryptoperidiniaceae, Peridinales), with evolutionary interpretations and a focus on the identity of *Durinskia oculata* from Prague. *Molecular Phylogenetics and Evolution*, 118, 392–402.
- Kretschmann, J., Žerdoner Čalasan, A., Meyer, B., & Gottschling, M. (2020). Zero intercalary plates in *Parvodinium* (Peridiniopsidaceae, Peridinales) and phylogenetics of *P. elpatiewskyi*, comb. nov. *Protist*, 171, 125700.
- Lajeunesse, T. C., Parkinson, J. E., & Reimer, J. D. (2012). A genetics-based description of *Symbiodinium minutum* sp. nov. and *S. psygmophilum* sp. nov. (Dinophyceae), two dinoflagellates symbiotic with Cnidaria. *Journal of Phycology*, 48, 1380–1391.
- Lefèvre, M. M. (1927). Sur les variations tabulaires chez les Péridiniens d'eau douce et leur notation. — Diagnoses d'espèces et de variétés nouvelles. *Bulletin Du Muséum National D'histoire Naturelle*, 33, 118–122.
- Lefèvre, M. M. (1932). Monographie des espèces du genre *Peridinium*. *Archives De Botanique*, 2, 1–210.
- Lemma, E. J. (1905). Beiträge zur Kenntnis der Planktonalgen. *Forschungsberichte aus der Biologischen Station zu Plön*, 12, 154–168.
- Lewis, J., & Dodge, J. D. (2011). Phylum Dinophyta (Dinoflagellates). In D. M. John, B. A. Whitton, & A. J. Brook (Eds.), *The freshwater algal flora of the British Isles: An identification guide to freshwater and terrestrial algae* (pp. 250–274). Cambridge: Cambridge University Press.
- Lindemann, E. B. L. W. (1916). *Peridinium Güstrowiense* n. sp. and seine Variationsformen. *Archiv Für Hydrobiologie*, 11, 490–495.
- Lindemann, E. B. L. W. (1917). Beiträge zur Kenntnis des Seenplanktons der Provinz Posen. (Südwestposener Seengruppe.) II. *Zeitschrift der Naturwissenschaftlichen Abteilung der Deutschen Gesellschaft für Kunst und Wissenschaft in Posen*, 24,3, 2–41.
- Lindemann, E. B. L. W. (1918). Mitteilungen über posener Peridineen. *Zeitschrift der Naturwissenschaftlichen Abteilung der Deutschen Gesellschaft für Kunst und Wissenschaft in Posen*, 25,1, 23–25.
- Lindemann, E. B. L. W. (1919). Untersuchungen über Süßwasserperidineen und ihre Variationsformen. *Archiv für Protistenkunde*, 39, 209–262.
- Lindemann, E. B. L. W. (1920). Untersuchungen über Süßwasserperidineen und ihre Variationsformen II. *Archiv für Naturgeschichte*, 84, 121–194.
- Lindemann, E. B. L. W. (1924). Peridineen des Alpenrandgebietes. *Botanisches Archiv*, 8, 297–303.
- Lindemann, E. B. L. W. (1931). Die Peridineen der deutschen limnologischen Sunda-Expedition nach Sumatra, Java und Bali. *Archiv für Hydrobiologie Suppl.*, 8, 691–732.
- Ling, H. U., Croome, R. L., & Tyler, P. A. (1989). Freshwater dinoflagellates of Tasmania, a survey of taxonomy and distribution. *British Phycological Journal*, 24, 111–129.
- Logares, R., Shalchian-Tabrizi, K., Boltovskoy, A., & Rengefors, K. (2007). Extensive dinoflagellate phylogenies indicate infrequent marine-freshwater transitions. *Molecular Phylogenetics and Evolution*, 45, 887–903.
- Luo, Z., Yang, W., Leaw, C. P., Pospelova, V., Bilien, G., Liow, G. R., et al. (2017). Cryptic diversity within the harmful dinoflagellate *Akashiwo sanguinea* in coastal Chinese waters is related to differentiated ecological niches. *Harmful Algae*, 66, 88–96.
- Mayr, E. (1982a). *The growth of biological thought : Diversity, evolution, and inheritance* (2nd ed.). Cambridge: Belknap.
- Mayr, E. (1982b). Of what use are subspecies? *The Auk*, 99, 593–595.
- Miller, M. A., Pfeiffer, W., & Schwartz, T. Creating the CIPRES Science Gateway for inference of large phylogenetic trees. *Proceedings of the Gateway Computing Environments Workshop (GCE), New Orleans, US-LA, 14 Nov. 2010* (pp. 1–8)
- Miller, S. E. (2007). DNA barcoding and the renaissance of taxonomy. *Proceedings of the National Academy of Science of the USA*, 104, 4775–4776.
- Minelli, A. (2019). The galaxy of the non-Linnaean nomenclature. *History and Philosophy of the Life Sciences*, 41, 31.
- Moestrup, Ø., & Calado, A. J. (2018). *Dinophyceae* (Vol. 6, Freshwater flora of Central Europe). Berlin: Springer.
- Montresor, M., Sgroso, S., Procaccini, G., & Kooistra, W. H. C. F. (2003). Intraspecific diversity in *Scrippsiella trochoidea* (Dinophyceae): Evidence for cryptic species. *Phycologia*, 42, 56–70.

- Netzel, H. (1982). Cytological and ecological aspects of morphogenesis and structure of recent and fossil protists-skeletons: Dinoflagellates. *Neues Jahrbuch für Geologie und Paläontologie Abhandlungen*, 164, 64–74.
- Olrik, K. (1992). Ecology of *Peridinium willei* and *P. volzii* (Dinophyceae) in Danish lakes. *Nordic Journal of Botany*, 12, 557–568.
- Pfiester, L. A. (1975). Sexual reproduction of *Peridinium cinctum* f. *ovoplanum* (Dinophyceae). *Journal of Phycology*, 11, 259–265.
- Pfiester, L. A. (1976). Sexual reproduction of *Peridinium willei* (Dinophyceae). *Journal of Phycology*, 12, 234–238.
- Pfiester, L. A. (1977). Sexual reproduction of *Peridinium gatunense* (Dinophyceae). *Journal of Phycology*, 13, 92–95.
- Pfiester, L. A., & Skvarla, J. J. (1979). Heterothallism and thecal development in the sexual life history of *Peridinium volzii* (Dinophyceae). *Phycologia*, 18, 13–18.
- Playfair, G. I. (1920). Peridiniaceae of New South Wales. *Proceedings of the Linnean Society of New South Wales*, 44, 793–818.
- Popovský, J., & Pfiester, L. A. (1990). *Dinophyceae (Dinoflagellida)* (Vol. 6, Süßwasserflora von Mitteleuropa). Stuttgart: Fischer.
- Romeikat, C., Izquierdo López, A., Tietze, C., Kretschmann, J., & Gottschling, M. (2019). Typification for reliable application of sub-specific names within *Peridinium cinctum* (Peridinales, Dinophyceae). *Phytotaxa*, 424, 147–157.
- Ronquist, F., Teslenko, M., van der Mark, P., Ayres, D. L., Darling, A., Höhna, S., et al. (2012). MrBayes 3.2: Efficient Bayesian phylogenetic inference and model choice across a large model space. *Systematic Biology*, 61, 539–542.
- Soyer-Gobillard, M. O., Bhaud, Y., & Saint Hilaire, D. (2002). New data on mating in an autotrophic dinoflagellate, *Prorocentrum micans* Ehrenberg. *Vie Et Milieu-Life and Environment*, 52, 167–175.
- Stamatakis, A. (2014). RAxML version 8: A tool for phylogenetic analysis and post-analysis of large phylogenies. *Bioinformatics*, 30, 1312–1313.
- Thornhill, D. J., & Lord, J. B. (2010). Secondary structure models for the Internal Transcribed Spacer (ITS) region 1 from symbiotic dinoflagellates. *Protist*, 161, 434–451.
- Tillmann, U., Bantle, A., Krock, B., Elbrächter, M., & Gottschling, M. (2021). Recommendations for epitypification of dinophytes exemplified by *Lingulodinium polyedra* and molecular phylogenetics of the Gonyaulacales based on curated rRNA sequence data. *Harmful Algae*, 104, 101956.
- Tillmann, U., Elbrächter, M., Krock, B., John, U., & Cembella, A. (2009). *Azadinium spinosum* gen. et sp. nov. (Dinophyceae) identified as a primary producer of azaspiracid toxins. *European Journal of Phycology*, 44, 63–79.
- Turland, N. (2019). *The Code decoded. A user's guide to the International Code of Nomenclature for algae, fungi, and plants* (2. ed., Advanced Books). Sofia: Pensoft.
- Wall, D., & Dale, B. (1968). Modern dinoflagellate cysts and evolution of Peridinales. *Micropaleontology*, 14, 265–304.
- Wang, N., Mertens, K. N., Krock, B., Luo, Z., Derrien, A., Pospelova, V., et al. (2019). Cryptic speciation in *Protoceratium reticulatum* (Dinophyceae): Evidence from morphological, molecular and eco-physiological data. *Harmful Algae*, 88, 101610.
- Warburton, F. E. (1967). The purposes of classifications. *Systematic Zoology*, 16, 241–245.
- West, G. S. (1909). The algae of the Yan Yean Reservoir, Victoria: A biological and ecological study. *The Journal of the Linnean Society of London. Botany*, 39, 1–88.
- Wong, B. B. M., & Candolin, U. (2015). Behavioral responses to changing environments. *Behavioral Ecology*, 26, 665–673.

**Publisher's Note** Springer Nature remains neutral with regard to jurisdictional claims in published maps and institutional affiliations in †Lingulodinium D. Wall (Tillmann et al., 2021).